Journal of ELECTRICAL ENGINEERING, VOL. 56, NO. 9-10, 2005, 225–236

DESIGN OF DECENTRALIZED ROBUST LFC IN A COMPETITIVE ELECTRICITY ENVIRONMENT

Hossein Shayeghi * — **Heidar Ali Shayanfar** **

A new decentralized robust controller for Load Frequency Control (LFC) in a deregulated electricity environment is presented in this paper. It is shown that subject to a condition based on the H_∞ norm and structured singular values (μ), each local area controller can be designed independently such that stability of the overall closed loop system is guaranteed. A generalized model for LFC scheme is developed based on the possible contracted scenarios. To achieve decentralization, the interfaces between control areas and the effects of load following contracts are treated as a set of new input disturbance signals in the control area dynamical model. In order to minimize the effects of the load disturbances under contract variations with large demand changes and to achieve desired level of robust performance in the presence of modeling uncertainties and practical constraints on control action the idea of mixed H_2/H_∞ control technique is used for solution of the LFC problem. This newly developed design strategy combines the advantage of the H_2 and H_∞ control synthesizes and gives a powerful multi-objectives design addressed by the Linear Matrix Inequality (LMI) techniques. The effectiveness of the proposed method is demonstrated on a three-area power system with possible contracted scenarios under large load demands. The results of the proposed controller are compared with the conventional PI controller and are shown to maintain robust performance in the presence of specified uncertainties and system nonlinearities.

K e y w o r d s: LFC, decentralized control, deregulated power system, mixed H_2/H_∞ control, robust control, LMI, large scale system

1 INTRODUCTION

In the dynamical operation of power systems, it is usually important to aim for decentralization of control action to individual areas. This aim should coincide with the requirements for stability and load frequency scheduling within the overall system. In a completely decentralized control scheme, the feedback controls in each area are computed on the basis of measurements taken in that area only. This implies that no interchange of information among areas is necessary for the purpose of Load Frequency Control (LFC). The advantages of this operating philosophy are apparent in providing cost savings in data communications and in reducing the scope of the monitoring network.

LFC provides a mechanism to balance generated power and demand in order to maintain the system frequency at the nominal value and to keep the power interchanges between neighbouring areas at the their scheduled values. In the deregulated environment, it will serve as ancillary service and acquires a principal role to provide better condition for electricity trading [1]. During the past decade several proposed LFC scenarios have attempted to adapt traditional LFC schemes to the change of environment in power system under deregulation [1–4].

LFC goals, *ie* frequency regulation and tracking the load demands, maintaining the tie-line power interchanges to specified values in the presence of modelling uncertainties, system nonlinearities and area load disturbances determines the LFC synthesis as a multi-objective optimization problem. Recently, several optimal and robust control strategies have been developed for LFC synthesis according to change of environment in power system operation under deregulation [5–9]. These methods show good dynamic response, but robustness in the presence of modelling uncertainties and system nonlinearities was not considered. Also, in most of the proposed robust methods, only one single norm is used to capture design specifications. It is clear that meeting all LFC design objectives by single control approach due to increasing the complexity and change of the power system structure is difficult.

In this paper, a new decentralized robust control strategy based on the mixed H_2/H_∞ control technique for LFC problem in a deregulated power system is proposed. This newly developed design strategy combines advantage of the H_2 and H_∞ control synthesizes to achieve the desired level of robust performance against load disturbances, modelling uncertainties, system nonlinearities and gives a powerful multi-objectives design addressed by the Linear Matrix Inequality (LMI) techniques [10].

It is shown that subject to a condition based on the H_∞ norm and structured singular values (μ), each local area controller can be designed independently such that stability of the overall closed loop system is guaranteed. The robust stability condition for the overall system can be easily stated as to achieve a sufficient interaction

* Technical Engineering Department, The University of Mohaghegh, Ardebil, Iran, h_ shayeghi@yahoo.com

** Electrical Engineering Department, Iran University of Science and Technology, Narmak, Tehran 16844, Iran, hashayanfar@yahoo.com

ISSN 1335-3632

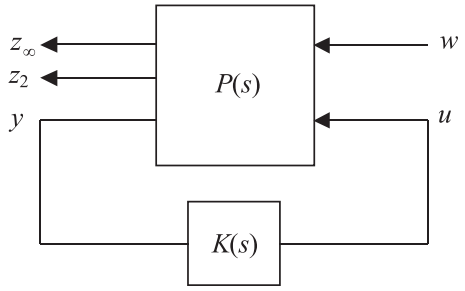

Fig. 1. The mixed H_2/H_∞ synthesis structure

margin, and a sufficient gain and phase margins during each independent design. Following the idea presented in [11] a generalized model for LFC scheme is developed based on the possible contracts in the deregulated environments. To achieve decentralization, the interface between areas and new inputs signals according to possible contracts on system dynamics are treated as a set of disturbance signals for each control area. Using the generalized model, the LFC problem is formulated as a decentralized multi-objective optimization control problem via a mixed H_2/H_∞ control technique and solved by the LMI approach to obtain the desired robust controllers.

The proposed control strategy is tested on a three-area power system and compared with the PI controller which is widely used in practical industries. To illustrate effectiveness of the proposed method two scenarios of possible contracts under large load demands have been simulated. The results show that the proposed controller guarantees the robust performance for a wide range of operating conditions in the presence of Generation Rate Constraints (GRC), modelling uncertainties and contract variations.

2 TECHNICAL BACKGROUND

In many real world control application, multi objectives such as stability, disturbance attenuation and reference tracking under model uncertainties and practical constraints are followed simultaneously. On the other hand, each robust control method is mainly useful to capture a set of special design specifications. For instance, noise attenuation or regulation against random disturbances is more naturally expressed in LQG terms (H_2 synthesis). Similarly, pure H_∞ synthesis is more useful for holding close- loop stability and formulation of some uncertainties and practical control constraints. It is shown that combination of H_2 and H_∞ (mixed H_2/H_∞) control techniques gives a powerful multi- objectives design including both sets of the above objectives. This section presents a brief overview of the mixed H_2/H_∞ via the LMI techniques. The synthesis problem is shown in Fig. 1, where $P(s)$ is a linear time invariant system with the following state-space realization.

$$\begin{aligned} \dot{\boldsymbol{x}} &= \mathbf{A}\boldsymbol{x} + \mathbf{B}_1\boldsymbol{w} + \mathbf{B}_2\boldsymbol{u} \\ \boldsymbol{z}_\infty &= \mathbf{C}_\infty\boldsymbol{x} + \mathbf{D}_{\infty 1}\boldsymbol{w} + \mathbf{D}_{\infty 2}\boldsymbol{u} \\ \boldsymbol{z}_2 &= \mathbf{C}_2\boldsymbol{x} + \mathbf{D}_{21}\boldsymbol{w} + \mathbf{D}_{22}\boldsymbol{u} \\ \boldsymbol{y} &= \mathbf{C}_y\boldsymbol{x} + \mathbf{D}_{y1}\boldsymbol{w} \end{aligned} \tag{1}$$

Where $\boldsymbol{x}$ is the state variable vector, $\boldsymbol{w}$ is the disturbance and other external vector and $\boldsymbol{y}$ is the measured output vector. The output channel $\boldsymbol{z}_\infty$ is associated with

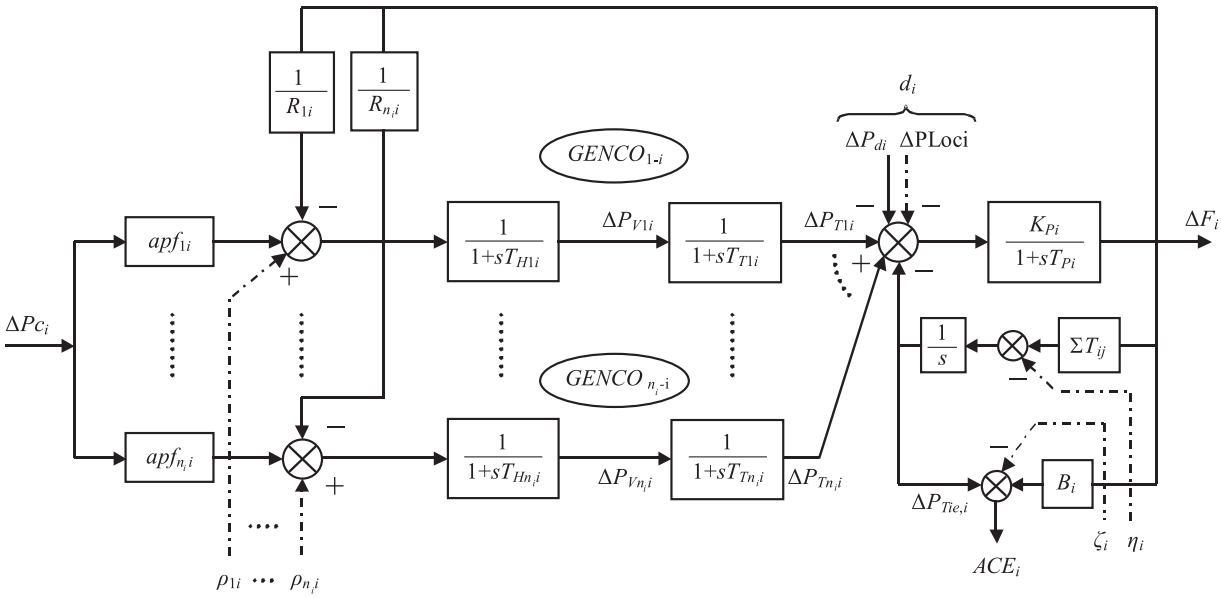

Fig. 2. Generalized LFC scheme for area i in the deregulated environment

the H_∞ performance, while the output channel $\boldsymbol{z}_2$ is associated with the H_2 performance.

Denoting by $T_\infty(s)$ and $T_2(s)$, the transfer functions from w to z_∞ and z_2, respectively, the mixed H_2/H_∞ synthesis problem can be expressed by the following optimization problem: design a controller $K(s)$ that minimize a trade off criterion of the form:

$$\alpha\|T_\infty(s)\|^2 + \beta\|T_2(s)\|^2 \quad (\alpha \geq 0, \beta \geq 0) \tag{2}$$

An efficient algorithm for solving this problem is available in LMI control toolbox of MATLAB [12]. The following lemmas relate the above optimization control problem to LMI techniques. Assume that the state-space realization of close loop system is given by:

$$\begin{aligned} \dot{\boldsymbol{x}} &= \mathbf{A}_{cl}\boldsymbol{x}_{cl} + \mathbf{B}_{cl}\boldsymbol{w} \\ \boldsymbol{z}_\infty &= \mathbf{C}_{cl\infty}\boldsymbol{x}_{cl} + \mathbf{D}_{cl\infty}\boldsymbol{w} \\ \boldsymbol{z}_2 &= \mathbf{C}_{cl2}\boldsymbol{x}_{cl} + \mathbf{D}_{cl2}\boldsymbol{w} \end{aligned} \tag{3}$$

LEMMA 1 (H_∞ performance) [13]. *The closed loop RMS gain for $T_\infty(s)$ does not exceed γ_∞ if and only if there exist a symmetric matrix $\mathbf{X}_\infty > 0$ such that:*

$$\begin{bmatrix} \mathbf{A}_{cl}\mathbf{X}_\infty + \mathbf{X}\mathbf{A}_{cl}^\top & \mathbf{B}_{cl} & \mathbf{X}_\infty\mathbf{C}_{cl}^\top \\ \mathbf{B}_{cl}^\top & -\mathbf{I} & \mathbf{D}_{cl\infty}^\top \\ \mathbf{C}_{cl\infty}\mathbf{X}_\infty & \mathbf{D}_{cl\infty} & -\gamma_\infty\mathbf{I} \end{bmatrix} < 0\,. \tag{4}$$

LEMMA 2 (H_2 performance) [13]. *The H_2 norm of $T_2(s)$ does not exceed γ_2 if and only if $\mathbf{D}_{cl2} = 0$ and there exist two symmetric matrices $\mathbf{X}_2$ and $\mathbf{Q}$ such that:*

$$\begin{bmatrix} \mathbf{A}_{cl}\mathbf{X}_2 + \mathbf{X}_2\mathbf{A}_{cl}^\top & \mathbf{B}_{cl} \\ \mathbf{B}_{cl}^\top & -\mathbf{I} \end{bmatrix} < 0\,,$$

$$\begin{bmatrix} \mathbf{Q} & \mathbf{C}_{cl2}\mathbf{X}_2 \\ \mathbf{X}_2\mathbf{C}_{cl2}^\top & \mathbf{X}_2 \end{bmatrix} > 0\,, \quad \mathrm{trace}(\mathbf{Q}) < \gamma_2^2\,. \tag{5}$$

The optimization control problem of Eq. (2) according to LMI techniques is solved using the function '*hinfmix*' in the LMI control toolbox of MATLAB [12].

3 GENERALIZED LFC SCHEME MODEL

In the deregulated power systems, the vertically integrated utility no longer exists, however, the common LFC objectives, *ie* restoring the frequency and the net interchanges to their desired values for each control area, still remain. The deregulated power system consists of three companies, Generation Companies (GENCOs), Transmissions Companies (TRANCOs) and Distribution Companies (DISCOs) with an open access policy. In the new structure, GENCOs may or may not participate in the LFC task and DISCOs have the liberty to contract with any available GENCOs in their own or other areas. Thus, various combinations of possible contracted scenarios between DISCOs and GENCOs are possible. All the transactions have to be cleared by the Independent System Operator (ISO) or other responsible organizations. Based on the idea presented in [11], the concept of an '*Augmented Generation Participation Matrix*' (AGPM) to express the possible contracts is presented here. The AGPM shows the participation factor of a GENCO in the load following contract with a DISCO for supplying power. The rows and columns of AGPM matrix equal the total number of GENCOs and DISCOs in the overall power system, respectively. Consider the number of GENCOs and DISCOs in area i be n_i and m_i in a large scale power system with N control area. The structure of AGPM is given by:

$$\mathbf{AGPM} = \begin{bmatrix} \mathbf{AGPM}_{11} & \dots & \mathbf{AGPM}_{1N} \\ \vdots & \ddots & \vdots \\ \mathbf{AGPM}_{N1} & \dots & \mathbf{AGPM}_{NN} \end{bmatrix} \tag{6}$$

where,

$$\mathbf{AGPM}_{ij} = \begin{bmatrix} gpf_{(s_i+1)(z_j+1)} & \cdots & gpf_{(s_i+1)(z_j+m_j)} \\ \vdots & \ddots & \vdots \\ gpf_{(s_i+n_i)(z_j+1)} & \cdots & gpf_{(s_i+n_i)(z_j+m_j)} \end{bmatrix},$$

$$\text{for } i, j = 1, \dots N; \text{ and}$$

$$s_i = \sum_{k=1}^{i-1} n_i\,,\; z_j = \sum_{k=1}^{j-1} m_j \;\&\; s_1 = z_1 = 0\,.$$

In the above, gpf_{ij} refer to *generation participation factor* and shows the participation factor GENCO i in total load following requirement of DISCO j based on the possible contract. The sum of all entries in each column of AGPM is unity. The diagonal sub-matrices of AGPM correspond to local demands and off-diagonal submatrices correspond to demands of DISCOs in one area to GENCOs in another area. Fig. 2 shows the block diagram of generalized LFC scheme for control area i in a restructured structure. The nomenclature used is given in Appendix. Dashed-dot lines show interfaces between areas and the demand signals based on the possible contracts. These new information signals were absent in the traditional LFC scheme. As there are many GENCOs in each area, ACE signal has to be distributed among them due to their ACE participation factor in the LFC task and $\sum_{j=1}^{n_i} apf_{ji} = 1$.

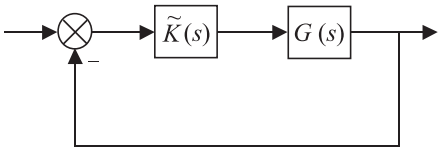

Fig. 3. An equivalent MIMO system

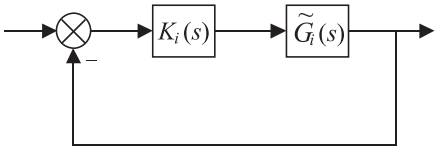

Fig. 4. Independent SISO system design

It can be seen from Fig. 2 that four input disturbance channels, d_i, ζ_i, η_i and ρ_i are considered for decentralized LFC design. They are defined as bellow:

$$d_i = \Delta P_{Loc,i} + \Delta P_{di}\,,$$

$$\Delta P_{Loc,i} = \sum_{j=1}^{m_i} \left(\Delta P_{Lj-i} + \Delta P_{ULj-i}\right) \tag{7}$$

$$\eta_i = \sum_{\substack{j=1 \\ j\neq i}}^{N} T_{i,j}\Delta f_j \tag{8}$$

$$\zeta_i = \sum_{\substack{k=1 \\ k\neq i}}^{N} \Delta P_{tie,ik,schudeled} \tag{9}$$

$$\Delta P_{tie,ik,schudeled} = \sum_{j=1}^{n_i}\sum_{t=1}^{m_k} apf_{(s_i+j)(z_k+t)}\Delta P_{L(z_k+t)-k} - \sum_{t=1}^{m_k}\sum_{j=1}^{m_i} apf_{(s_k+t)(z_i+j)}\Delta P_{L(z_i+j)-i} \tag{10}$$

$$\Delta P_{tie,i-error} = \Delta P_{tie,i-actual} - \zeta_i \tag{11}$$

$$\rho_i = \left[\rho_{1i}\dots\rho_{ki}\dots\rho_{n_i i}\right]^\top, \quad \rho_{ki} = \Delta P_{m,k-i} \tag{12}$$

$$\Delta P_{m,k-i} = \sum_{j=1}^{z_{N+1}} gpf_{(s_i+k)j}\Delta P_{Lj-i} + apf_{ki}\sum_{j=1}^{m_i}\Delta P_{ULj-i},\ k = 1,2,\dots,n_i \tag{13}$$

$\Delta P_{m,k-i}$ is the desired total power generation of a GENCO k in area i and must track the demand of the DISCOs in contract with it in the steady state. Due to Fig. 2, the state space model for area i can be obtained as:

$$\begin{aligned} \dot{\boldsymbol{x}}_i &= \mathbf{A}_i\boldsymbol{x}_i + \mathbf{B}_{iu}\boldsymbol{u} + \mathbf{B}_{iw}\boldsymbol{w}_i' \\ \boldsymbol{y}_i &= \mathbf{C}_i\boldsymbol{x}_i + \mathbf{D}_{iw}\boldsymbol{w}_i' \end{aligned} \tag{14}$$

where,

$$\boldsymbol{x}_i^\top = [x_{ai}x_{1i}\dots x_{ki}\dots x_{n_i i}]\,, \boldsymbol{x}_{ai} = [\Delta f_i\ \Delta P_{tie,i}]$$

$$x_{ki} = [\Delta P_{Tki}\ \Delta P_{Vki}]\,,\ \boldsymbol{u}_i = \Delta P_{ci}\,,\ \boldsymbol{y}_i = ACE_i$$

$$\boldsymbol{w}_i' = [d_i\ \eta_i\ \xi_i\ \rho_i]^\top,\ \rho_i = [\rho_{1i}\dots\rho_{ki}\dots\rho_{n_i i}]$$

$$\mathbf{A}_i = \begin{bmatrix} \mathbf{A}_{11i} & \mathbf{A}_{12i} \\ \mathbf{A}_{21i} & \mathbf{A}_{22i} \end{bmatrix},\ \mathbf{A}_{11i} = \begin{bmatrix} 1/T_{Pi} & -K_{Pi}/T_{Pi} \\ \sum_{\substack{j=1 \\ j\neq i}}^{N} T_{ji} & 0 \end{bmatrix}$$

$$\mathbf{A}_{12i} = \underbrace{\left[\begin{pmatrix} K_{Pi}/T_{Pi} & 0 \\ 0 & 0 \end{pmatrix} \dots \begin{pmatrix} K_{Pi}/T_{Pi} & 0 \\ 0 & 0 \end{pmatrix}\right]}_{n_i \text{ blocks}}$$

$$\mathbf{A}_{21i} = \left[DP_{1i}^\top \dots DP_{ki}^\top \dots DP_{n_i i}^\top\right],$$

$$\mathbf{A}_{22i} = \operatorname{diag}\left(TG_{1i},\dots,TG_{ki},\dots,TG_{n_i i}\right)$$

$$DP_{ki} = \begin{bmatrix} 0 & 0 \\ -1/(R_{ki}T_{Hki}) & 0 \end{bmatrix},$$

$$TG_{ki} = \begin{bmatrix} -1/T_{Tki} & 1/T_{Tki} \\ 0 & -1/T_{Hki} \end{bmatrix}$$

$$\mathbf{B}_{iu}^\top = \left[0_{2\times 1}^\top\ \mathbf{B}_{1iu}^\top \dots \mathbf{B}_{kiu}^\top \dots \mathbf{B}_{n_i iu}^\top\right],$$

$$\mathbf{B}_{kiu} = [0\ apf_{ki}/T_{Hki}]^\top$$

$$\mathbf{B}_{iw}^\top = \left[\mathbf{B}_{aiw}^\top\ B_{1iu}^\top \dots B_{kiw}^\top \dots B_{n_i iw}^\top\right]$$

$$\mathbf{B}_{kiw} = \begin{bmatrix} -K_{Pi}/T_{Pi} & 0 & 0_{1\times(n_i+1)} \\ 0 & -1 & 0_{1\times(n_i+1)} \end{bmatrix}$$

$$\mathbf{B}_{kiw} = \begin{bmatrix} 0_{1\times 3} & 0 & \dots & 0 & \dots & 0 \\ 0_{1\times 3} & b_{1i} & \dots & b_{ki} & \dots & b_{n_i i} \end{bmatrix},$$

$$b_{ji} = \begin{cases} -1/T_{Hki} & j = i \\ 0 & j \neq i \end{cases}$$

$$\mathbf{C}_i = [C_{ai}\ 0_{1\times 2n_i}]\,,$$

$$\mathbf{C}_{ai} = [B_i\ 1]\,,\ \mathbf{D}_{iw} = [0_{1\times 2} \quad -1 \quad 0_{1\times n_i}]$$

4 DECENTRALIZED CONTROLLER DESIGN

A centralized controller design is often considered not feasible for large-scale systems such as power system; in turn decentralized control is adopted. The advantages of a decentralized controller design are reduction in the controller complexity and suitability for practical implementation. In the next subsections, the problem of decentralized load frequency controller is translated into an equivalent problem of decentralized control design for a Multi-Input, Multi-Output (MIMO) control system. The proposed method is based on the H_∞ norm and structured singular value (μ).

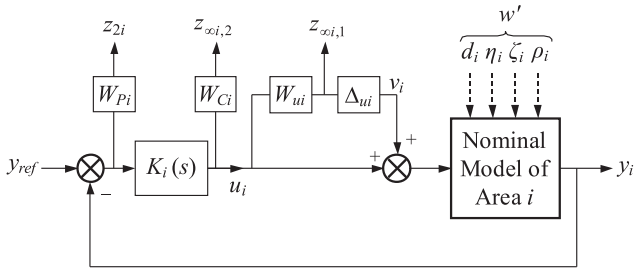

Fig. 5. The proposed synthesis framework

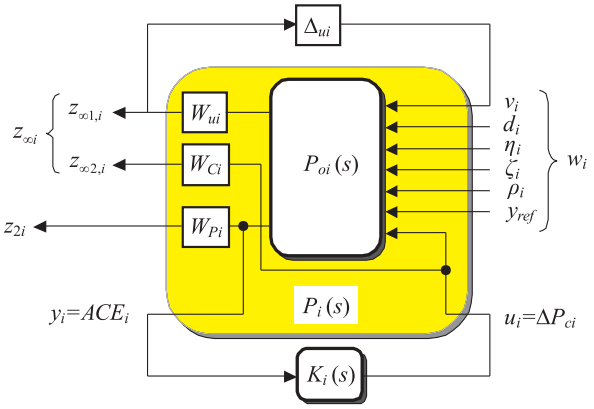

Fig. 6. The formulation of mixed H_2/H_∞ based control design problem

4.1 Problem Formulation

In general, an N-area power system LFC problem can be modelled as a large-scale power system consisting of N subsystems:

$$\begin{aligned} \dot{\boldsymbol{x}} &= \mathbf{A}_N \boldsymbol{x} + \mathbf{B}_N \boldsymbol{u} \\ \boldsymbol{y} &= \mathbf{C}_N \boldsymbol{x} \end{aligned} \tag{15}$$

where $\boldsymbol{u} = [u_1, \ldots, u_N]^\top$; $\boldsymbol{y} = [y_1, \ldots, y_N]^\top$; $\boldsymbol{x} = [x_1, \ldots, x_N]^\top$ and x_i are the state variables for the ith area as given in Eq. (14). Equivalently, this system composed of N linear time-invariant subsystem $G_i(s)$, described by:

$$\begin{aligned} \dot{x}_i &= A_{ii} x_i + \sum_{\substack{j=1 \\ j \neq i}} A_{ij} x_j + B_{ii} u_i \\ y_i &= C_{ii} x_i \end{aligned} \tag{16}$$

It assume that all (A_{ii}, B_{ii}) are controllable, (A_{ii}, C_{ii}) are observable and all A_{ii} and C_{ii} are full rank. The term $\sum_{\substack{j=1 \\ j \neq i}}^{N} A_{ij} x_j$ is due to the interconnections other subsystems. An $N \times N$ transfer function matrix $G(s)$ linking $U(s) = [u_1(s), \ldots, u_N(s)]^\top$ and $Y(s) = [y_1(s), \ldots, y_N(s)]^\top$:

$$Y(s) = G(s) U(s)\,. \tag{17}$$

It can be calculated as:

$$G(s) = \mathbf{C}_N (s\mathbf{I} - \mathbf{A}_N)^{-1} \mathbf{B}_N\,. \tag{18}$$

The design of N decentralized local controllers now becomes the design of an $N \times N$ diagonal matrix $\tilde{K}(s) = \mathrm{diag}\{K_i(s)\}$, $i = 1, \ldots, N$, as shown in Figs. 3 and 4.

If all A_{ij} $(i \neq j)$ in $G_i(s)$ were equal to zero, then each controller could be designed independently just as if it were in a SISO system as shown in Fig. 4. However, since A_{ij} $(i \neq j)$ are not zeros, the following question must be resolved, *ie* if each $K_i(s)$ $(i = 1, \ldots, N)$ is designed to form a stable closed loop system as shown in Fig. 4, what are the additional conditions which can guarantee that the overall system of Fig. 3 is stable? The answer to this questions is discussed in the next subsection based on the theorem given by Labibi and *et al* [14].

4.3 Stability Condition

In Labibi's paper, $\widetilde{G}(s)$ is considered as the matrix consisting of the diagonal elements of $G(s)$; *ie* :

$$\widetilde{G}(s) = \mathrm{diag}\big\{\widetilde{G}_1(s), \widetilde{G}_2(s), \ldots, \widetilde{G}_N(s)\big\} \tag{19}$$

Where $\widetilde{G}_i(s)$ is the ith diagonal element of the transfer function matrix $G(s)$ and has the following state-space realization:

$$\begin{aligned} \dot{\boldsymbol{x}}_i &= \mathbf{A}_{ii} \boldsymbol{x}_i + \mathbf{B}_{ii} \boldsymbol{u}_i \\ \boldsymbol{y}_i &= \mathbf{C}_{ii} \boldsymbol{x}_i \end{aligned} \tag{20}$$

Using the notations:

$$\widetilde{K}(s) = \mathrm{diag}\big\{K_i(s)\big\} = \mathrm{diag}\big\{K_1(s), K_2(s), \ldots, K_N(s)\big\} \tag{21}$$

$$\widetilde{A} = \mathrm{diag}\big\{A_{ii}\big\} = \mathrm{diag}\big\{A_{11}, A_{22}, \ldots, A_{NN}\big\} \tag{22}$$

$$A_d = A - \widetilde{A} \tag{23}$$

Labibi *et al* have proved the following theorem:

The close loop overall system is stable if:

c1) The decentralized controller $\widetilde{K}(s)$ stabilizes the diagonal system $\widetilde{G}(s)$.

c2) $\rho_{\max} < \mu^{-1}(A_d)$.
where, $\rho_{\max} = \max_i \big\{ \big\| (sI - A_{ii} + B_{ii} K_i(s) C_{ii})^{-1} \big\|_\infty$, $\|\cdot\|_\infty$ is the H_∞ norm and μ denotes Doyle's SSV.

This theorem gives sufficient conditions for the stability of the overall closed loop system. However, Authors have shown that although (c2) may has some conservativeness compared the diagonal dominant and the generalized diagonal dominant conditions, it gives the tightest restrictive band and is less conservative than the one proposed by the Grosdidier and Morari [15].

Before applying the above results to our system it is necessary to consider the issue of the robust stability. The stability condition (c2) is given for the nominal

plant $G(s)$. If the state space model of Eq. (15) changes, the plant model of $G(s)$ will also change. It is generally not possible to establish a clear relationship between the change of values in Eq. (15) and the change of values involved in condition (c2). For this reason, we specify the stability conditions as:

r1) Condition (c2) is satisfied with a sufficient margin. This is can be checked by computing $\rho_{\max}$ and $\mu^{-1}(A_d)$ and an Interaction Margin (IM) that can be defined as the difference between values of $\mu^{-1}(A_d)$ and $\rho_{\max}$.

r2) There are sufficient gain and phase margins in each SISO loop for the stability. This can also be checked by a Bode or Nyquist plot of $K_i(s)\widetilde{G}_i(s)$.

5 MIXED H_2/H_∞ BASED LFC FORMULATION

LFC goals, *ie* frequency regulation and tracking the load demands, maintaining the tie-line power interchanges to specified values in the presence of modelling uncertainties, system nonlinearities and area load disturbances determines the LFC synthesis as a multi-objective optimization problem. For this reason, the idea of mixed H_2/H_∞ control synthesis which gives a powerful multi-objectives design is used for solution of this problem. The main synthesis framework to formulate it as a mixed H_2/H_∞ control design for a given control area (Fig. 2) is shown in Fig. 5.

In deregulated power systems, each control area contains different kinds of uncertainties because of plant parameter variations, load changes and system modelling errors due to some approximations in model linearization and unmodelled dynamics. Usually, the uncertainties in power system can be modelled as multiplicative and/or additive uncertainties [16]. In Fig. 5 the Δu_i block models the unstructured uncertainties as a multiplicative type and Wu_i is the associated weighting function. The output channels $z_{\infty i,1}$ and $z_{\infty i,2}$ are associated with H_∞ performance. The first channel is used to meet robustness against uncertainties and reduce their impacts on close loop system performance. In the second channel $(z_{\infty i,2})$, W_{Ci} sets a limit on the allowed control signal to penalize fast change and large overshoot in the control action signal with regard to practical constraints. The output channel z_{2i} is associated with the H_2 performance and W_{pi} sets the performance goal *ie* zero tracking error and minimizing the effects of disturbances on the area control error (ACE_i). We can redraw the Fig. 5 as a mixed H_2/H_∞ general framework synthesis as shown in Fig. 6, where $P_{0i}(s)$ and $K_i(s)$ denote the nominal area model as given by Eq. (14) and controller, respectively. Also, y_i is the measured output (performed by ACE_i), u_i is the control output and w_i includes the perturbed, disturbance and reference signals in the control area.

In Fig. 6, $P_i(s)$ is the Generalized Plant (GP) that includes nominal models of control area i and associated weighting functions. The state-space model of GP can be obtained as:

$$\begin{aligned}
\dot{\boldsymbol{x}}_{GPi} &= \mathbf{A}_{GPi}\boldsymbol{x}_{GPi} + \mathbf{B}_{1i}\boldsymbol{w}_i + \mathbf{B}_{2i}\boldsymbol{u}_i \\
\boldsymbol{z}_{\infty i} &= \mathbf{C}_{\infty i}\boldsymbol{x}_{GPi} + \mathbf{D}_{\infty 1i}\boldsymbol{w}_i + \mathbf{D}_{\infty 2i}\boldsymbol{u}_i \\
\boldsymbol{z}_{2i} &= \mathbf{C}_{2i}\boldsymbol{x}_{GPi} + \mathbf{D}_{21i}\boldsymbol{w}_i + \mathbf{D}_{22i}\boldsymbol{u}_i \\
\boldsymbol{y}_i &= \mathbf{C}_{yi}\boldsymbol{x}_{GPi} + \mathbf{D}_{y1i}\boldsymbol{w}_i
\end{aligned} \tag{24}$$

where,
$\boldsymbol{w}_i^\top = [\, v_i \quad d_i \quad \eta_i \quad \xi_i \quad \rho_i \quad y_{\mathrm{ref}} \,]$, $\boldsymbol{z}_{\infty i}^\top = [\, z_{\infty 1i} \quad z_{\infty 2i} \,]$.

Now, the synthesis problem is: designing a controller $K_i(s)$ as shown in Fig. 6 such that Eq. (2) is minimized. This optimization problem is solved using the *hinfmix* function in the LMI control toolbox, which gives an optimal controller to achieve the desired level of robust performance. In summary, the designing steps of the proposed method are:

Step 1: Compute the state space model for the given control area. This can be obtained based on the Eq. (14) as given in Sec. 3.

Step 2: Identify the uncertainty (W_{ui}) and performance weighting functions (W_{Pi} and W_{Ci}) for the given control area. For more details on how these weighting functions are chosen refer to Sec. 5.

Step 3: Problem formulation as a general mixed H_2/H_∞ control structure according to Fig. 6 and obtaining state space model of GP (Eq. (24)). This can be constructed using the function 'sysic' in μ-analysis and synthesis toolbox [17].

Step 4: Identify the indexes α, β and solve optimization problem in Eq. (2) using the '*hinfmix*' function of LMI control toolbox to obtain the desired controller.

Step 5: Reduce the order of resulted controller by using standard model reduction techniques. See [18] for more details.

It is should be noted that the order of the designed controller by this strategy is the same as size of the generalized plant that is typically high in general. In order to overcome the complexity of computation in the case of high order power systems, appropriated model reduction techniques might be applied to the obtained controller model.

The design strategy includes enough flexibility to set the desired robust performance and is a decentralized LFC scheme, which requires only the ACE. Thus, its construction and implementation are relatively easy and can be used in the real world power systems.

6 CASE STUDY

A three control area power system, shown in Fig. 7 is considered as a test system to illustrate effectiveness of the proposed control strategy. It is assumed that one area has three GENCOs and two DISCOs and others have two GENCOs and one DISCO. The power systems parameters are given in Tables 1 and 2.

Table 1. GENCOs parameter

MVA_{base} (1000MW) Parameter	GENCOs (k in area i)						
	1–1	2–1	3–1	1–2	2–2	1–3	2–3
Rate (MW)	1000	800	1000	1100	900	1000	1020
T_T (sec)	0.40	0.4	0.42	0.44	0.40	0.40	0.41
T_H (sec)	0.08	0.08	0.07	0.06	0.08	0.07	0.08
R (Hz/pu)	3	3	3.3	2.73	2.5	3	2.94
apf	0.4	0.4	0.2	0.6	0.4	0.5	0.5

Table 2. Control area parameters

Parameter	Area–1	Area–2	Area–3
K_P (Hz/pu)	120	120	125
T_P (sec)	20	25	20
B (pu/Hz)	0.3375	0.3966	0.3522
T_{ij} (pu/Hz)	$T_{12} = 0.272, T_{13} = 0.212$		

Simulation results and eigenvalue analysis show that the open loop system performance is affected more significantly by changing in the K_{pi}, T_{pi}, B_i and T_{ji} than changes of other parameters. Thus, is assumed that these parameters have uncertain values in each control area. Hence, for the given power system, we have set our objectives to area frequency regulation and assuring robust stability and performance in the presence of specified uncertainties, load disturbances or exogenous inputs as follows:

1. Holding stability and robust performance for the overall power system and each control area in the presence of 25 % uncertainty for the K_{pi}, T_{pi}, B_i and T_{ji}.
2. Minimizing the effects of new input signals according to possible contracts and area interfaces $(\eta_i, \zeta_i\, \rho_i)$ on the output signals.
3. Getting zero steady state error and good tracking for load demands and disturbances.
4. Maintaining acceptable overshoot and settling time on the frequency deviation signal in each control area.
5. Setting the reasonable limit on the control action signal from the change speed and amplitude view point.

Following, we will discuss application of the proposed strategy on the given power system to achieve the above objectives for each of the three control areas separately. Because of similarity and to save space, the first controller synthesis will be described in detail and for the other control areas, only the final results will be presented.

6.1 Uncertainty Weights Selection

As it is mentioned in the previous section, we can consider the specified uncertainty in each area as a multiplicative uncertainty associated with a nominal model. Let $\widehat{P}_i(s)$ denote the transfer function from the control input u_i to control output y_i at operating points other than the nominal point. Following a practice common in robust control, this transfer function will be represented as:

$$\begin{aligned} &|\Delta u_i(s) W_i(s)| = \left|\left(\widehat{P}_i(s) - P_{0i}(s)/P_{0i}(s)\right)\right|;\ P_{0i}(s) \neq 0 \\ &\left\|\Delta u_i(s)\right\|_\infty = \sup\left|\Delta u_i(s)\right| \leq 1 \end{aligned} \tag{25}$$

Where, $\Delta u_i(s)$ shows the uncertainty block corresponding to the uncertain parameters and $P_{0i}(s)$ is the nominal transfer function model. Thus, $W_{ui}(s)$ is such that its magnitude Bode plot covers the Bode plot of all possible plants. Using Eq. (25) some sample uncertainties corresponding to different values of K_{pi}, T_{pi}, B_i, and T_{ji} are shown in Fig. 8 for one area. It can be seen that multiplicative uncertainties have a peak around the 5.5 rad/s. Based on this figure the following multiplicative uncertainty weight was chosen for control design as:

$$W_{u1} = \frac{3.0449s^2 + 7.6083s + 18.9308}{s^2 + 0.37725s + 30.6716}\,. \tag{26}$$

Fig. 8 clearly shows that attempting to cover the sharp peak around the 5.5 rad/s will result in large gaps between the weight and uncertainty at other frequencies. On the other hand a tighter fit at all frequencies using a higher order transfer function will result in a high order controller. The weight (26) used in our design gives a conservative design around the 5.5 rad/s, low and high frequency, but it provides a good trade off between robustness and controller complexity. Using the same method, the uncertainty weighting function for area 2 and 3 are calculated as follows:

$$\begin{aligned} W_{u2} &= \frac{1.9666s^2 + 5.6379s + 11.6588}{s^2 + 1.1549s + 21.3477} \\ W_{u3} &= \frac{2.0209s^2 + 5.8804s + 11.8491}{s^2 + 1.1647s + 19.677} \end{aligned} \tag{27}$$

6.2 Performance Weights Selection

The selection of performance weights W_{Ci} and W_{Pi} entails a trade off among different performance requirements, particularly good area control error minimization versus peak control action. The weight on the control input, W_{Ci}, must be chosen close to a differentiator to penalize fast change and large overshoot in the control input due to corresponding practical constraints. The weight on the output, W_{Pi}, must be chosen close to an integrator at low frequency in order to get disturbance rejection and zero steady state error. More details on how these weights are chosen are given in [19–20]. Based on the above discussion, a suitable set of performance weighting functions for one control area is chosen as:

$$W_{C1} = \frac{0.3s + 1}{s + 10}\,, \quad W_{P1} = \frac{0.03s + 0.75}{235s + 1} \tag{28}$$

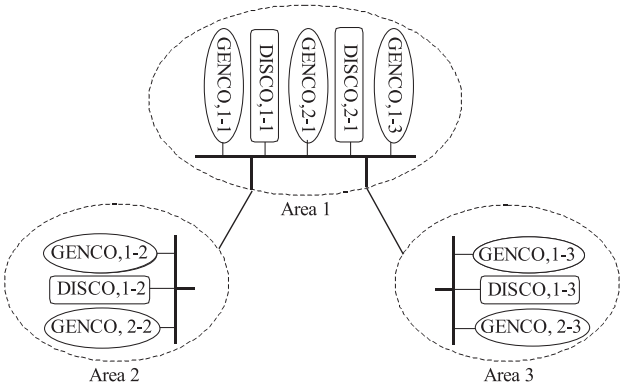

Fig. 7. Three area power system

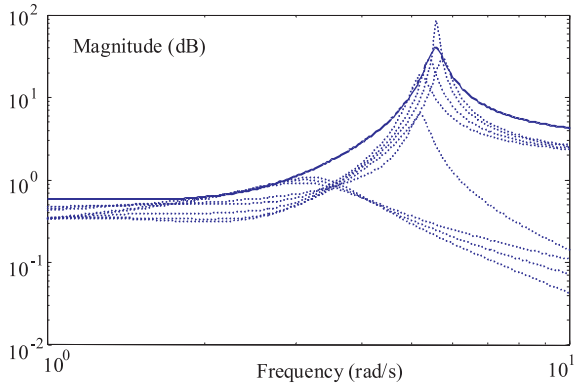

Fig. 8. Uncertainty plot due to change of K_{pi}, T_{pi}, B_i and T_{ji} (Dotted) and $W_{ui}(s)$ (Solid)

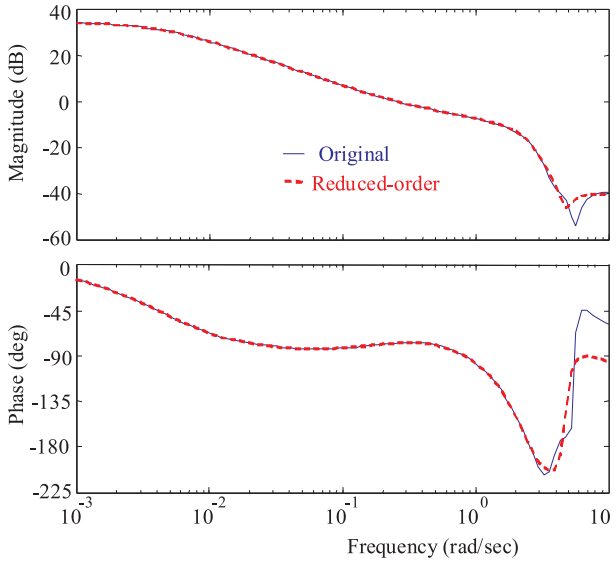

Fig. 9. Bode plot comparison of original and reduced order controller $K_1(s)$

6.3 Mixed H_2/H_∞ Control Design

Based on the problem formulation in Sec. 5 and synthesis methodologies in Sec. 2, a decentralized robust controller is designed for one control area using the *hinfmix* function in the LMI control toolbox. This function gives an optimal controller through the mentioned optimization problem Eq. (2) with α and β fixed at unity. The resulting controller is dynamic type and whose order is the same as the size of the GP model (here 10). The order of controller is reduced to a 4 with no performance degradation using the standard Hankel norm approximation. The Bode plots of the full order and reduced order controllers are shown in Fig. 9. The transfer function of the reduced order controller with simple structure is given as:

$$K_1(s) = 1.1 \times 10^{-1} \frac{s^3 + 0.667s^2 + 22.903s + 7.967}{s^4 + 2.882s^3 + 6.854s^2 + 4.075s + 0.017} \tag{29}$$

Using the same procedure and setting similar objectives as discussed above the set of suitable weighting function for the other control area synthesis are given in Table 3. The resulting controllers can be approximated by low order controllers as follows:

$$\begin{aligned} K_2(s) &= 1.29 \times 10^{-1} \frac{s^3 + 2.12s^2 + 14.398s + 4.889}{s^4 + 3.69s^3 + 6.786s^2 + 4.254s + 4.889} \\ K_3(s) &= 3.77 \times 10^{-1} \frac{s^3 + 1.548s^2 + 14.481s + 2.296}{s^4 + 4.213s^3 + 8.338s^2 + 2.99s + 0.024} \end{aligned} \tag{30}$$

6.4 Stability Analysis

In this subsection, stability of the overall system with the proposed decentralized Mixed H_2/H_∞ based controllers is investigated. Due to discussion as mentioned in Sec. 4 state space realization of the overall system can be constructed as:

$$\begin{aligned} \dot{\boldsymbol{x}} &= \mathbf{A}\boldsymbol{x} + \mathbf{B}\boldsymbol{u} \\ \boldsymbol{y} &= \mathbf{C}\boldsymbol{x} \end{aligned} \tag{31}$$

Where $\boldsymbol{u} = [u_1 \;\; u_2 \;\; u_3]^\top$; $\boldsymbol{y} = [y_1 \;\; y_2 \;\; y_3]^\top = [ACE_1 \;\; ACE_2 \;\; ACE_3]^\top$; $\boldsymbol{x} = [x_1 \;\; x_2 \;\; x_3]^\top$ and x_i is the state variables for ith area as given in Eq. (14), $\mathbf{A} \in R^{20\times 20}$, $\mathbf{B} \in R^{20\times 3}$, $\mathbf{C} \in R^{3\times 20}$;

$$\mathbf{A} = \begin{bmatrix} \mathbf{A}_{11} & \mathbf{A}_{12} & \mathbf{A}_{13} \\ \mathbf{A}_{21} & \mathbf{A}_{22} & \mathbf{A}_{23} \\ \mathbf{A}_{31} & \mathbf{A}_{32} & \mathbf{A}_{33} \end{bmatrix}$$

$$\mathbf{B} = \text{blockdiag}\big(\mathbf{B}_{11}, \mathbf{B}_{22}, \mathbf{B}_{33}\big);$$

$$\mathbf{C} = \text{blockdiag}\big(\mathbf{C}_{11}, \mathbf{C}_{22}, \mathbf{C}_{33}\big)$$

$\mathbf{A}_{ii}$, $\mathbf{B}_{ii}$ and $\mathbf{C}_{ii}$ are the same as $\mathbf{A}_i$, $\mathbf{B}_{iu}$, $\mathbf{C}_i$ as given in Eq. (14). The $\mathbf{A}_{ij}$ is given by:

$$\mathbf{A}_{ij} = [a_{ij}]_{i=1,\ldots,n_i\,;\,j=1,\ldots,n_j}$$

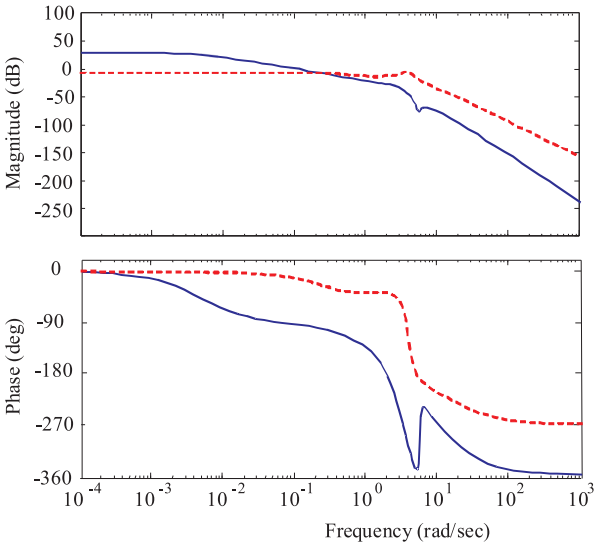

Fig. 10. Bode plot of $K_1(s)\widetilde{G}_1(s)$ (solid line) and $\widetilde{G}_1(s)$ (dashed line)

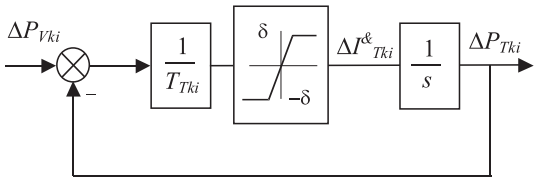

Fig. 11. A nonlinear turbine model with GRC

Table 3. The set of performance weighting functions

Weight	Area–2	Area–3
W_{Pi}	$\frac{0.01s+0.65}{200s+1}$	$\frac{0.01s+0.6}{120s+1}$
W_{Ci}	$\frac{0.3s+1}{s+10}$	$\frac{0.3s+1}{s+10}$

Table 4. Gain and phase margins

	$\widetilde{G}_i(s)$		$K_i(s)\widetilde{G}_i(s)$	
	GM (dB)	PM (deg)	GM (dB)	PM (deg)
Loop 1 (Area–1)	7.85	42.59	19.39	79.72
Loop 2 (Area–2)	12.10	63.41	19.62	90.52
Loop 3 (Area–3)	13.19	70.62	15.06	86.88

Where n_i and n_j are the number of state variables area i and j, respectively ($n_1 = 8$, $n_2 = 6$, $n_3 = 6$). The all entries of $\mathbf{A}_{ij}$ is zero except the a_{21} is $-T_{ij}$.

Using the decentralized controllers given in pervious subsection and the formulae mentioned in section 4 the IM defined before is obtained as: 26.5 dB.

The frequency response of $\widetilde{G}_1(s)$ and $K_1(s)\widetilde{G}_1(s)$ is shown in Fig. 10. The Gain Margin (GM) is increased from 7.85 dB to 19.39 dB and the Phase Margin (PM) is increased from 42.59 to 79.72°. The improvements each individual loop's GM and PM are listed in Table 4 for the other areas.

The above results show that with the proposed decentralized controllers robust stability of the overall power system is achieved and the system performance is significantly improved.

7 SIMULATION RESULTS

In the simulation study, the linear model of a turbine $\Delta P_{VKi}/\Delta P_{TKi}$ in Fig. 2 is replaced by a nonlinear model of Fig. 11 (with ±0.03 limit). This is to take GRC into account, *ie* the practical limit on the rate of change in the generating power of each GENCO. Simulations are carried out for two scenarios in the presence of large load demands, uncertainties and disturbances. The performance of the proposed method is compared with the conventional PI controller which is widely used in practical Industries.

7.1 Scenario 1

In this scenario, the closed loop performance is tested in the presence both step contracted load demands and uncertainties. It is assumed that a large step load is demanded by all DISCOs as follow:

$\Delta P_{L1\text{–}1} = 100$, $\Delta P_{L2\text{–}1} = 80$, $\Delta P_{L1\text{–}2} = 100$, $\Delta P_{L1\text{–}3} = 50$ MW

A case of combined Poolco and bilateral based contracts between DISCOs and available GENCOs is simulated based on the following AGPM.

$$AGPM^{\top} = \begin{bmatrix} 0.25 & 0.5 & 0 & 0 & 0.25 & 0 & 0 \\ 0 & 0.5 & 0.25 & 0 & 0 & 0 & 0.25 \\ 0.5 & 0 & 0 & 0.25 & 0.25 & 0 & 0 \\ 0 & 0 & 0 & 0 & 0 & 1 & 0 \end{bmatrix}$$

All GENCOs participate in the LFC task. The one GENCO in areas 2 and 3 only participate for performing the LFC in their areas, while other GENCO track the load demand in their areas and/or others. Power system responses with 25 % decrease in uncertain parameters K_{Pi}, T_{Pi}, B_i and T_{ij} are depicted in Figs. 12 and 13. Using the proposed method, the frequency deviation of all areas is quickly driven back to zero and the tie-line power flow properly converges to the specified value of Eq. (10) in the steady state. i.e:

$\Delta P_{tie,21,sch} = -0.025$, $\Delta P_{tie,31,sch} = 0.02$ pu MW

Also, the actual generated powers of GENCOs properly reached the desired values in the steady state as given by Eq. (13). i.e.:

$\Delta P_{m,1\text{–}1} = 0.075$, $\Delta P_{m,2\text{–}1} = 0.09$, $\Delta P_{m,3\text{–}1} = 0.02$ pu MW

$\Delta P_{m,1\text{–}2} = 0.025$, $\Delta P_{m,2\text{–}2} = 0.05$ pu MW

$\Delta P_{m,1\text{–}3} = 0.05$, $\Delta P_{m,2\text{–}3} = 0.02$ pu MW

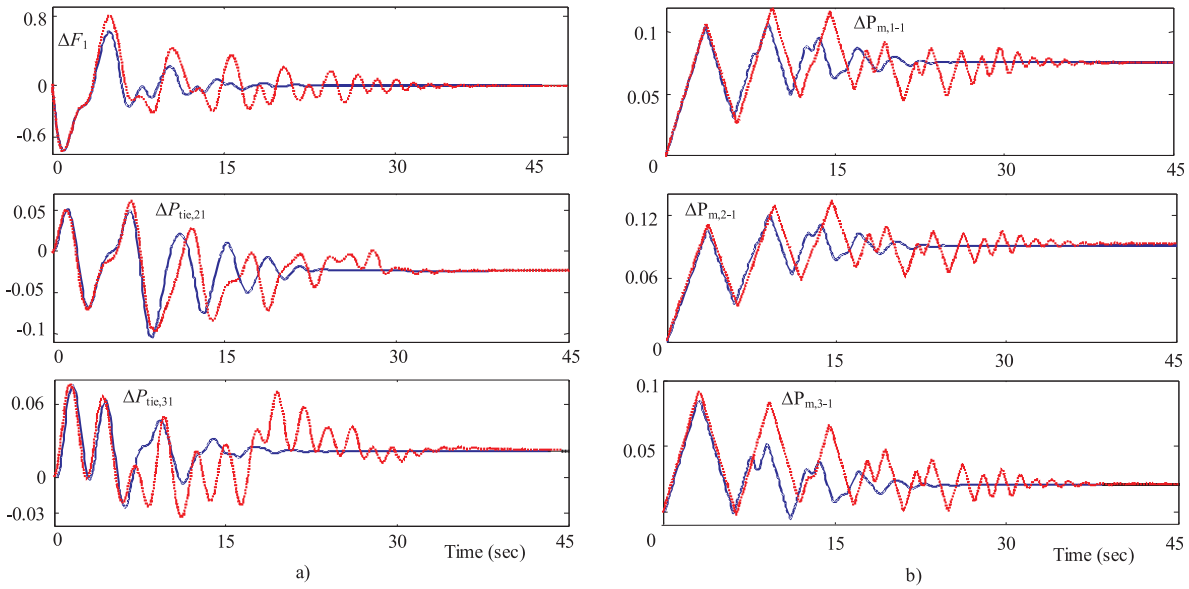

Fig. 12. a) Frequency deviation in area1 and tie line power deviation b) GENCOs Power changes in area 1; Solid (Mixed H_2/H_∞) and Dotted (PI)

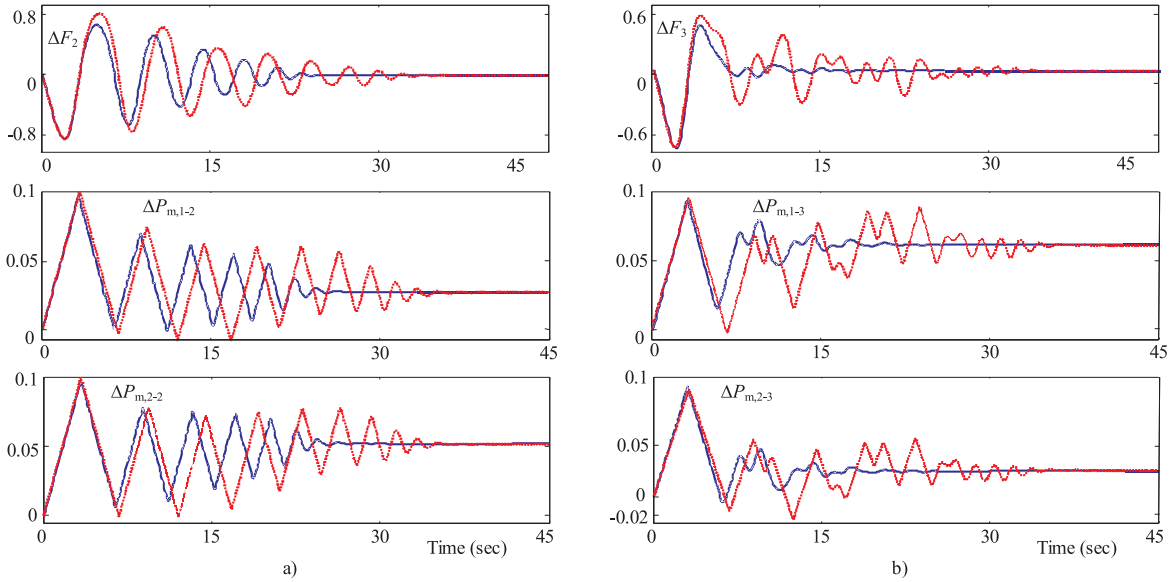

Fig. 13. Frequency deviation and GENCOs Power changes a) Area 2 b) Area 3; Solid (Mixed H_2/H_∞) and Dotted (PI)

7.2 Scenario 2

In this case, DISCO may violate a contract by demanding more power than that specified in the contract. This excess power is reflected as a local load of the area (uncontracted load). Consider scenario 1 again. It is assumed that in addition to specified contracted load demands and 25 % decrease in uncertain parameters, area 2 DISCO's demands 0.1 pu MW as a large uncontracted load.

Using the Eq. (7), the total local load in all areas is obtained as:

$\Delta P_{Loc,1} = 0.18,\ \Delta P_{Loc,2} = 0.2,\ \Delta P_{Loc,3} = 0.05$ pu MW

The purpose of this scenario is to test the effectiveness of the proposed controller against uncertainties and large load disturbances in the presence of GRC. The power system responses for areas 1 and 2 are shown in Fig. 14. Using the proposed method, the frequency deviation of these areas is quickly driven back to zero and the tie-line power flows properly converge to value specified by Eq. (10) in the steady state. As AGPM is the same as in scenario 1 and the uncontracted load of area 2 is taken up by the GENCOs in the same area, the tie-line power is the same as in scenario 1 in the steady state (Fig. 14b).

The un-contracted load of $\text{DISCO}_{1\text{–}2}$ is taken up by the GENCOs in area 2 according to ACE participation factors in the steady state. Using the Eq. (13) the actual generated power of GENCOs in area 2 is given by:

$\Delta P_{m,1\text{–}2} = 0.085,\ \Delta P_{m,2\text{–}2} = 0.09$ pu MW

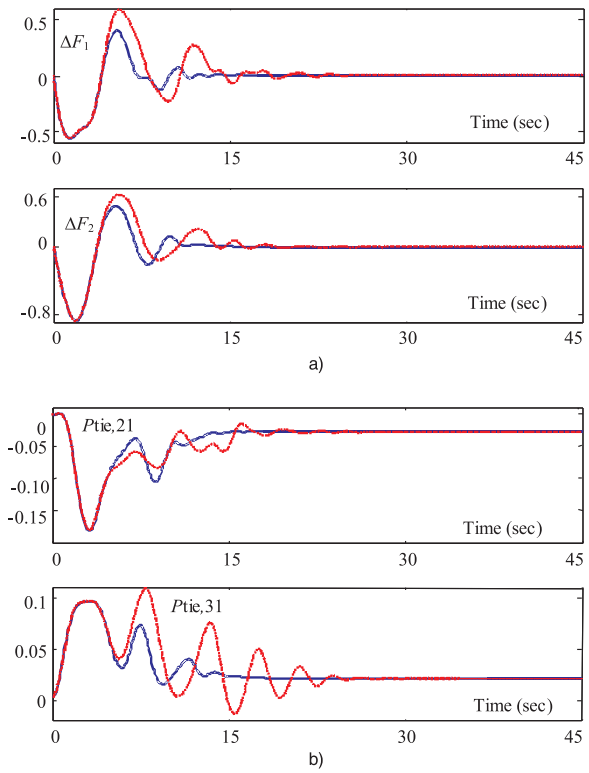

Fig. 14. a) Frequency deviation b) Tie line power changes, Solid (Mixed H_2/H_∞) and Dotted (PI)

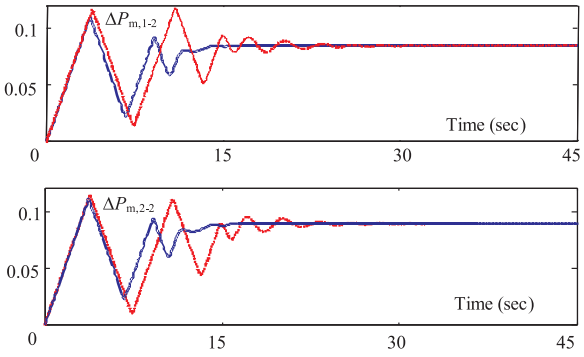

Fig. 15. GENCOs Power changes in area 2; Solid (Mixed H_2/H_∞) and Dotted (PI)

As shown in Fig. 15, the actual generated powers of GENCOs properly reached the desired values using the proposed strategy.

8 CONCLUSION

A new decentralized robust controller for LFC in a deregulated power system using the generalized LFC scheme is proposed in this paper. It has been shown that subject to a condition based on the H_∞ norm and structured singular values (μ), each local area controller can be designed independently such that stability of the overall closed loop system is guaranteed. Since, each control area in the deregulated power system contains different kinds of uncertainties and disturbances because of increasing the complexity and change of power system structure. Thus, the LFC problem has been formulated as a decentralized multi-objective optimization control problem via a mixed H_2/H_∞ control approach and solved by LMI techniques to obtain optimal controller. Synthesis problem introduce appropriate uncertainties to consider of practical limits, has enough flexibility for setting the desired level of robust performance and leads to a set of simple controllers, which are ideally practical for the real world complex power systems. The effectiveness of the proposed strategy was tested on a three-area power system and compared with the PI controller under possible contracts with various load changes in the presence of modelling uncertainties and GRC. The simulation results show that the proposed method achieve good robust performance such as frequency regulation, tracking the load changes and disturbances attenuation under possible contracts and a wide range of area load disturbances than the PI controller.

Appendix: Nomenclature

F	area frequency
P_{Tie}	net tie-line power flow
P_T	turbine power
P_V	governor valve position
P_C	governor set point
ACE	area control error
apf	ACE participation factor
Δ	deviation from nominal value
K_P	subsystem equivalent gain
T_P	subsystem equivalent time constant
T_T	turbine time constant
T_H	governor time constant
R	droop characteristic
B	frequency bias
T_{ij}	tie line synchronizing coefficient between area i and j
P_d	area load disturbance
P_{Lj-i}	contracted demand of Disco j in area i
P_{ULj-i}	uncontracted demand of Disco j in area i
$P_{m,j-i}$	power generation of GENCO j in area i
P_{Loc}	total local demand
η	area interface
ζ	scheduled power tie line power flow deviation

References

[1] JALEELI, N.—VANSLYCK, L. S.—EWART, D. N.—FINK, L. H.—HOFFMANN, A. G.: Understanding Automatic Generation Control, IEEE Trans. On Power Systems **7** No. 3 (1992), 1106–1122.

[2] KUMAR, J.—HOE, N. G.—SHEBLE, G.: AGC Simulator for Price-Based Operation Part I: Modeling, IEEE Trans. on Power Systems **12** No. 2 (1997), 527–532.

[3] CHRISTIE, R. D.—BOSE, A.: Load Frequency Control Issues in Power System Operations after Deregulation, IEEE Trans. on Power Systems **11** No. 3 (1996), 1191–1200.

[4] FELIACHI, A.: On Load Frequency Control in a Deregulated Environment,, IEEE Inter. Conf. on Control Applications, pp. 437-441, 15–18 Sept. 1996.

[5] BEVRANI, H.—MITANI, Y.—TSUJI, K.: Robust Decentralized AGC in a Restructured Power System, Energy Conversion and Management **45** (2004), 2297–2312.

[6] LIU, F.—SONG, Y. H.—MA, J.—LU, Q.: Optimal Load Frequency Control in Restructured Power Systems, IEE Proc. On Gen. Trans. Dis. **150** No. 1 (2003), 87–95.

[7] RERKPREEDAPONG, D.—HASANOVIC, A.—FELIACHI, A.: Robust Load Frequency Control Using Genetic Algorithms and Linear Matrix Inequalities, IEEE Trans. on Power Systems **18** No. 2 (2003), 855–861.

[8] TYAGI, B.—SRIVASTAVA, S. C.: A Fuzzy Logic Based Load Frequency Controller in a Competitive Electricity, IEEE Power Engineering Society General Meeting, vol. 2, pp. 560–565, 2003.

[9] RERKPREEDAPONG, D.—FELIACHI, A.: Decentralized Load Frequency Control for Load Following Services, IEEE Power Engineering Society Winter Meeting, vol. 2, pp. 1252–1257, 2002.

[10] SCHERER, C.—GAHINET, P.—CHILALI, M.: Multi-objective Output-Feedback Control via LMI Optimization, IEEE Trans. on Automatic Control **42** No. 7 (1997), 896–911.

[11] DONDE, V.—PAI, A.—HISKENS, I.. A.: Simulation and Optimization in a AGC System after Deregulation, IEEE Trans. on Power Systems **16** No. 3 (2001), 481–489.

[12] GAHINET, P.—NEMIROVSKI, A.—LAUB, A. J.—CHILALI, M.: LMI Control Toolbox, The Mathworks Inc., South Natick, 1995.

[13] SCHERER, C. W.: Multi-objective Mixed H_2/H_∞ Control, IEEE Trans. on Automatic Control **40** No. 2 (1995), 1054–1062.

[14] LABIBI, B.—LOHMANN, B.—KHAKI SEDIGH, A.—JABEDAR MARALANI, P.: Output Feedback Decentralized Control of Large-Scale Systems Using Weighted Sensitivity Functions Minimization, Systems and Control Letters **47** (2002), 191–198.

[15] GROSDIDIER, P.—MORARI, M.: Interaction Measures for System under Decentralized Control, Automatica **22** No. 3 (1986), 309–319.

[16] DJUKANOVIC, M. B.—KHAMMASH, M. H.—VITTAL, V.: Sensitivity Based Structured Singular Value Approach to Stability Robustness of Power Systems, IEEE Trans. on Power Systems **15** No. 2 (2000), 825–830.

[17] BALAS, G. J.—DOYLE, J. C.—GLOVER, K.—PAKARD, A.—SMITH, R.: The μ-Analysis and Synthesis Toolbox for Use with MATLAB, The Mathworks Inc., South Natick, 1998.

[18] SKOGESTED, S.—POSTLETHWAITE, I.: Multivariable Feedback Control, John Wiley & Sons, 1996, pp. 449–467.

[19] SHAYEGHI, H.—KARRARI, M.: Theory of μ Synthesis for Power Systems Load Frequency Control, J. Electrical Engineering **51** (2000), 258–263.

[20] ZHOU, K. DOYLE, J. C.: Essentials of Robust Control, Prentice-Hall, Englewood Cliffs, New Jercy, 1998, pp. 88–94.

Received 11 April 2005

Hossein Shayeghi received the BS and MSE degrees in Electrical Engineering from KNT and Amirkabir Universities of Technology in 1996 and 1998, respectively. He is currently a PhD candidate at the Iran University of Science and Technology (IUST), Tehran, Iran. His research interests are in the application of robust control, artificial intelligence to power system control design and power system restructuring. He is a member of Iranian Association of Electrical and Electronic Engineers (IAEEE) and a student member of IEEE.

Heidar Ali Shayanfar received the BS and MSE degrees in Electrical Engineering in 1973 and 1979 and the PhD degree in Electrical Engineering from Michigan State University, USA, in 1981. Currently, he is a Full Professor at Electrical Engineering Department of IUST, Tehran, Iran. His research interests are in the application of artificial intelligence to power system control design, dynamic load modelling, power system observability studies and voltage collapse. He is a member of Iranian Association of Electrical and Electronic Engineers (IAEEE) and IEEE.